

# Modelling the number counts of early-type galaxies by pure luminosity evolution

Ping He<sup>2</sup> and Yuan-Zhong Zhang<sup>1,2</sup>

<sup>1</sup>*CCAST (World Laboratory), P.O.Box 8730, Beijing 100080, P.R.China*

<sup>2</sup>*Institute of Theoretical Physics, Academia Sinica, P.O.Box 2735, Beijing 100080, P.R.China (hemm@itp.ac.cn)*

## ABSTRACT

In this paper, we explore the plausible luminosity evolution of early-type galaxies in different cosmological models by constructing a set of pure luminosity evolution (PLE) models via the choices of the star formation rate (SFR) parameters and formation redshift  $z_f$  of galaxies, with the observational constraints derived from the Hubble Space Telescope (HST) morphological number counts for elliptical and S0 galaxies of the Medium Deep Survey (MDS) and the Hubble Deep Field (HDF). We find that the number counts of early-type galaxies can be explained by the pure luminosity evolution models, without invoking exotic scenarios such as merging or introducing an additional population. But the evolution should be nearly passive, with a high  $z_f$  assumed. The conclusion is valid in all of the three cosmological models we adopted in this paper. We also present the redshift distributions for three bins of observed magnitudes in F814w pass-band, to show at which redshift are the objects that dominate the counts at a given magnitude. The predictions of the redshift distribution of  $22.5 < b_j < 24.0$  are also presented for comparison with future data.

**Key words:** galaxies: elliptical and lenticular, cd - galaxies: evolution - galaxies: luminosity function, mass function - cosmology: miscellaneous.

## 1 INTRODUCTION

One of the most basic astronomical methods is to simply count the number of galaxies as a function of apparent magnitude. Such exploration can be traced back to the early work of Hubble (Hubble 1926), and revived in the seventies after a nearly half century's gap (Brown & Tinsley 1974). Ever since then, it has been widely-used to probe the evolutionary history of galaxy populations, or to help estimate the parameters of cosmological geometry. It is just these attempts that brought about a problem called the excess of faint blue galaxies (FBGs), which remains one of the grand astronomical issues for a long time (Koo & Kron 1992, Ellis 1997). The difficulties lie in that one cannot find a logically simple and self-consistent way to explain the observational data of different aspects. If one tries to reproduce deep blue galaxy counts using flat faint-end luminosity functions (LFs), with no evolution (nE) assumed, the observed number counts show an excess with respect to the expected predictions by a factor of  $\sim 4$  to  $5$  at  $b_j \sim 24$ , rising up by a factor of  $\sim 5$  to  $10$  at  $b_j \sim 26$  (Maddox et al. 1990a; Guiderdoni & Rocca-Volmerange 1991), and continuously increasing to the faintest levels observed at  $b_j \sim 28$ . The adoption of an open geometry can moderate, but still not help ameliorate the situation. The introduction of pure luminosity evolution (PLE), which, as a natural consideration,

allows the spectra and luminosity of galaxies to change with redshifts, can provide a better fit to the faint galaxy number counts in the  $b_j$  pass-band, if an open geometry ( $q_0 < 0.5$ ) or a cosmological constant ( $\Lambda > 0$ ) is involved (Broadhurst, Ellis & Shanks 1988; Colless et al. 1990; Cowie, Songaila & Hu 1991; Colless et al. 1993; Fukugita et al. 1990). But as infrared photometric data become available, one finds that  $K$ -band ( $2.2\mu\text{m}$ ) counts show no excess with respect to the no-evolution predictions up to  $K \sim 21$  (Cowie et al. 1990; Gardner, Cowie & Wainscoat 1994), and such PLE models will overpredict the counts in  $K$ -band (Cowie 1991). On the other hand, the PLE models also overpredict a high- $z$  distribution of galaxies, which is not found in the results of  $z$  surveys of faint galaxies (Broadhurst et al. 1988; Colless et al. 1990; Koo & Kron 1992 and references therein). To get away from such a dilemma (i.e., the optical/infrared and the photometric/spectroscopic paradoxes), a number of less straitforward models concerning number evolution of galaxies have been proposed. One is the merger model which would decrease the comoving number density of objects while increasing their luminosities (Guiderdoni & Rocca-Volmerange 1991; Broadhurst, Ellis & Glazebrook 1992; Carlberg & Charlot 1992; Kauffmann, Guiderdoni & White 1994). Another is to introduce an entirely new population of dwarf galaxies which once existed in early times and have faded and/or disappeared in recent epochs (Broad-

hurst et al. 1988; Cowie 1991; Cowie et al. 1991; Babul & Rees 1992; Babul & Ferguson 1996).

Another complexity we need to consider is that there may exist some inherent uncertainties in the present-day LFs, which is not well-determined by the local surveys. For instance, if we adopt a high normalization of the characteristic density, or consider a steep faint-end-slope, which may accommodate more dwarf galaxies than the flat one, the degree of excess will be substantially decreased (Saracco, Chincarini & Iovino 1996). An extensive investigation of literature shows that there exist many discrepancies between different research groups (cf. King & Ellis 1985; Loveday et al. 1992; Marzke et al. 1994a, 1994b; Im et al. 1995; Roche et al. 1996) in the determination and/or adoption of the values of the luminosity function (LF) parameters ( $\phi^*$ ,  $M^*$ ,  $\alpha$ ) and the relative mix ratio between different morphological types. Some authors (De Propris et al. 1995) even announced that an extreme steep slope of LF faint-end had been observed, say  $\alpha \sim -2.2$ , in the cores of four rich clusters of galaxies (Abell 2052, Abell 2107, Abell 2199 and Abell 2666). The uncertainties in local LFs include, e.g., a large local fluctuation (Shanks 1989), significant local evolution (Maddox et al. 1990b), selection effects and/or incompleteness (Zwicky 1957; Disney 1976; Ferguson & McGaugh 1995), or perhaps systematic errors in local surveys (Metcalfe, Fong & Shanks 1995). Thus the universality of LFs is doubtful, while the well-determination of present-day LF is of great significance for understanding the galaxy evolution at high redshifts, and is conducive to reconciling the paradoxes mentioned previously.

Great progress of observational cosmology in recent years has been made through the powerful ground-based 10 –  $m$  Keck telescope, and especially the Hubble Space Telescope (HST). The latter, with its high resolution of 0.1'' FWHM, can provide us with image information of great value in that the morphologies of different Hubble types can be segregated into several wide classes (cf. Driver & Windhorst 1995a; Driver et al 1995b; Abraham et al. 1996, and references therein). With morphological data, it becomes possible to simplify the modelling of FBGs so that each morphological type can be allowed to be modelled independently, and hence the complexity of each individual model can be greatly reduced (Driver & Windhorst 1995a).

Following this line of thought, we consider first the modelling of E/S0's number counts in the Medium Deep Survey (MDS) and the Hubble Deep Field (HDF) obtained by WFPC2's F814w pass-band on board HST in the present paper, by means of PLE models according to the latest version of population synthesis models of Bruzual & Charlot (1997, hereafter BC97), without invoking the more exotic scenarios mentioned above. We choose the parameters of the star formation rates (SFRs) and the formation redshift ( $z_f$ ) of galaxies to reproduce the photometric properties such as colors and spectral energy distributions (SEDs) of the local population. Another motivation of this paper is to explore up to what extent the parameters of cosmological models within the framework of standard cosmology can be constrained by our PLE models. We find that the number count-magnitude relation of E/S0 galaxies can be well explained by our PLE model in any cosmological geometry we adopted in this paper, including a)  $\Omega_0=1$ ,  $h=0.5$  ( $H_0=100h$  km s<sup>-1</sup> Mpc<sup>-1</sup>), b)  $\Omega_0=0.1$ ,  $h=0.5$  and c)  $\Omega_0=0.2$ ,  $\lambda_0=0.8$ ,

$h = 0.6$ , under the appropriate choice of the parameters of SFRs and  $z_f$ s. This seems to be conflicting with the result of Drive et al. (1996).

In Section 2 we will demonstrate the basic methods for modelling the number counts by pure luminosity evolution of galaxies and describe the cosmological models as well as the LF for early-type galaxies adopted in this work. Some details such as dust extinction are also introduced. The results of our models are shown in Section 3 for comparison with the observational data. In Section 4, we will discuss the influence of uncertainties in LF, dust extinction and different initial mass function (IMF) upon our results. A comparison of our work with others is also made in this section. We will give our summary and conclusions in Section 5.

## 2 MODELLING THE NUMBER COUNTS OF ELLIPTICALS

The number distribution of galaxies between the interval  $(m, z) \sim (m + dm, z + dz)$  is stated by the expression as follows:

$$d^2N(m_\lambda, z) = \frac{\omega}{4\pi} \frac{dV}{dz} \phi(M_\lambda) dm_\lambda dz, \quad (1)$$

where  $\omega$  is solid angle,  $dV$  is the comoving volume element of the redshift interval  $z \sim z + dz$ , and  $\phi$  is the present-day LF. The relation between apparent magnitude  $m$  and  $M$  in the  $\lambda$ -pass band is given by

$$m_\lambda = M_\lambda + 5 \log\left(\frac{d_L}{10}\right) + corr, \quad (2)$$

where  $d_L$  is the luminosity distance measured in  $pc$  and dependent on cosmology. The term *corr* refers to the correction needed to translate the galaxy observer-frame magnitude into its rest-frame magnitude. In the nE model, it is only characterized by  $k$ -correction, which accounts for the red-shifting of the spectra due to the recession of galaxies. The  $e$ -correction should be considered if the intrinsic galaxy luminosity evolution is involved, and in more realistic cases, some secondary effects, e.g., dust extinction, should also be taken into account to some extent. The magnitude-limited number counts ( $z$ -distribution) can be obtained by integrating (1) over the specific magnitude range  $(m_1, m_2)$ . By integrating over redshift  $z$  the differential number counts (number-magnitude relation) of galaxies can be obtained. Since galaxies will become drastically faint beyond the redshift  $z_L$  at which the Lyman continuum break is shifted into the effective wavelength of the pass-band being considered (Madau 1995), the upper limit of the integral over  $z$  should be  $z_{up} = \min(z_f, z_L)$ , where  $z_f$  is the assumed  $z$  of galaxy formation. For  $B$ -band  $z_L$  is 4.0, while for F814w it is 7.8. We will see the significance of this consideration in what follows.

### 2.1 Cosmological Models

As one of the goals of our present exploration, we would examine the validity of our PLE models under the three choices of the currently popular cosmological models. The first we consider is  $\Omega_0=1$  and  $H_0=50$  km s<sup>-1</sup> Mpc<sup>-1</sup>, a flat Einstein-de Sitter universe favoured by the standard inflation theory. The second we adopted is the Friedmann-Robertson-Walker model, in which we adopt  $\Omega_0=0.1$ ,  $H_0=50$  km s<sup>-1</sup> Mpc<sup>-1</sup>,

**Table 1.** Parameters of the cosmological models under consideration, as well as the assumed formation redshifts of galaxies.

Scenario	$h^a$	$\Omega_0$	$\lambda_0$	$z_f^b$
A	0.5	1.0	0	3.5, 5, 8, 10
B	0.5	0.1	0	2.5, 3.5, 5, 10
C	0.6	0.2	0.8	2.5, 3.5, 5, 10

<sup>a</sup>  $H_0 = 100h \text{ km s}^{-1} \text{ Mpc}^{-1}$ ;

<sup>b</sup>  $z_f$  refers to the redshift of galaxy formation.

representing the low density universe. The third is  $\Lambda$ -dominated Friedmann-Lemaître model for which we choose  $\lambda_0=0.8$ ,  $\Omega_0=0.2$  and a higher Hubble constant  $H_0=60 \text{ km s}^{-1} \text{ Mpc}^{-1}$ , also compatible with the inflation theory. Both the low density and the  $\Lambda$ -dominated universes have larger volumes at a given redshift. We list the parameters of these cosmological models in Table 1. Also listed in it are the galaxy formation redshifts we assumed in the three cosmological models.

Once a specific cosmological model is given, the relations between redshifts, look-back times and volume elements, which are needed in modelling, can be determined completely by the standard formulae (cf. Weinberg 1972; Guiderdoni & Rocca-Volmerange 1990; Fukugita et al. 1990).

## 2.2 Evolutionary SEDs of Galaxies

There are standard evolutionary synthesis techniques (Bruzual & Kron 1980; Guiderdoni & Rocca-Volmerange 1987; Charlot & Bruzual 1991; Bruzual & Charlot 1993, hereafter BC93; Bruzual & Charlot 1997, hereafter BC97) to obtain the SEDs of galaxies. Our galaxy SEDs are computed on the basis of the latest galaxy isochrone synthesis spectral evolution library (GISSEL96, BC97). The BC97 models are built from a library of stellar tracks in the theoretical H-R diagram, covering all evolutionary stages of stars with multi-metallicity. The spectra of galactic stars, from near-UV to near-IR, extending to the far-UV by means of model atmospheres, are employed in the synthesis. For the present purpose, however, we do not model the evolution of metallicity with respect to  $z$ , and consider the solar metallicity only.

Colors of galaxies, as a significant photometric property, can provide us with valuable information about their present-day composition of stars, and accordingly give us important clues to the formation and evolution of galaxies. In the present work, we use several broad-band colors of elliptical galaxies (see Table 2) observed locally as the preliminary constraints on our selections of the model parameters. The photometric systems we use here are: Johnson's *UBVRI* systems (Johnson & Morgan 1953), Couch's  $b_j$  and  $r_f$  (Couch & Newell 1980) and the Palomar 200 IR detectors'  $K$  band filter (effective wavelength,  $2.2 \mu\text{m}$ ). We set the photometric zero point by the SEDs of the star of  $\alpha$  Lyre. Thus we can compute the model colors to make comparison with the observed ones, and among them we select the SFR parameters to give the best fit.

Throughout this work, we adopt the Scalo (1986) IMF for our models. The Scalo IMF is less rich in massive stars

**Table 2.** Observed colors of local elliptical and S0 galaxies for reference.

CI	observed
$U - B^a$	0.43
$B - V^a$	0.95
$B - R^b$	1.83
$b_j - I^c$	2.39
$b_j - K^b$	4.16

<sup>a</sup> Mixed from Fukugita et al. (1995);

<sup>b</sup> Mixed from Yoshii et al. (1988);

<sup>c</sup> Mixed from Yoshii et al. (1988) and Lidman et al. (1996).

than the Salpeter (1955) IMF because of the steeper slope of the former at the high-mass end. By the adoption of Scalo IMF, the UV flux of early times can be greatly reduced so as to avoid a large number of galaxies being detected at high  $z$ , which are not observed in current deep surveys (Pozzetti, Bruzual & Zamorani 1996, hereafter PBZ96).

## 2.3 Dust Extinction

Simple luminosity evolution models (e.g., PBZ96) only consider the contributions to the fluxes by star populations. But in reality, most galaxies are full of interstellar medium (ISM), and hence effects of internal absorption by dust are also needed to be introduced into the modelling. In particular, the dust extinction has great influence upon  $z$ -distributions of galaxies (Wang 1991; Gronwall & Koo 1995; Campos & Shanks 1995).

Unlike the situation in spiral galaxies, however, physical and evolutionary relationships between the various components of the ISM in ellipticals are not yet well understood (Goudfrooij, 1996). To circumvent the complexity and uncertainty in determining the law of extinction for ellipticals, we make an *ad hoc* assumption that Wang's prescription, which is just the simulation for spirals, could be extrapolated to the description of dust extinction for ellipticals, except that we choose a larger geometrical parameter  $\zeta=0.50$ , and a smaller optical depth  $\tau_{z=0} = 0.10$ , in  $B$ -band for present-day  $L^*$  ellipticals, which mimic the geometrical feature and less dust content for local ellipticals, in contrast with the adoption by Wang, that  $\zeta = 0.25$  and  $\tau_{z=0} = 0.20$  for spirals. We also assume that the optical depth depends on the galaxy luminosity as  $\tau \propto L_{z=0}^{0.5}$ , which is a simple representation of the fact that luminous galaxies are seen to be much dustier than those of lower luminosity. The extinction curve of our models is taken to be a power law in wavelength, namely  $\propto \lambda^{-n}$ , with  $n = 2$  (Draine & Lee 1984), which is the same as Wang's adoption. By such choices, the extinctions for  $B$ -band are 0.05 mag at present-day, and 1.02 mag at  $z = 5$ ; for F814w they are 0.02 and 0.50 at  $z = 0$  and 5, respectively. Observationally, extinction corrections in  $B$  band for ellipticals in the nearby 4 clusters are 0.18mag (A2256,  $z=0.0601$ ), 0.07mag (A2029,  $z=0.077$ ), 0.05mag (Coma,  $z=0.023$ ), and 0.04mag (A957,  $z=0.045$ ), obtained from the NASA Extragalactic Database (cf. Schade, Barrientos & López-Cruz 1997). Hence, the results of our models can be accepted when compared with the

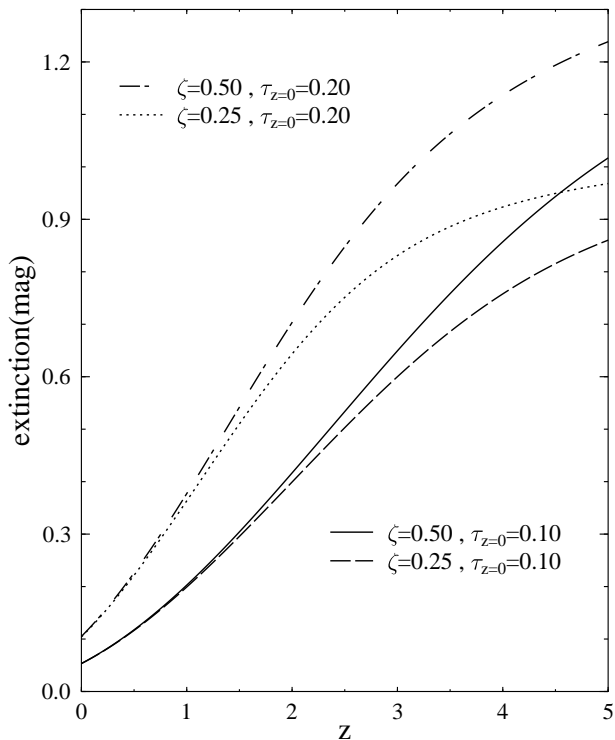


**Figure 1.** Extinction in the  $B$ -band as a function of redshift for an  $L^*$  galaxy. The predictions of models are shown by lines, with the model parameters (see Wang 1991 for denotations of these parameters) exhibited in the figure.

observation. We show the relation of extinction against redshift in  $B$ -band in Figure 1. It can be seen that present-day extinctions are not affected by the geometrical parameter  $\zeta$ , but are sensitive to the local optical depth  $\tau_{z=0}$ ; while  $\zeta$  will play an important role at high redshifts, at which fluxes are greatly reduced, and hence galaxies become much fainter by a thick geometrical parameter than the thin one.

Needless to say, it is only a simple treatment, since we do not model the dust evolution and some other details such as the inclination of galaxies are also neglected. But even so, the effect of dust extinction can greatly reduce the UV flux in early epochs due to the wavelength dependence on the extinction law.

## 2.4 Luminosity Function

The present-day luminosity function of galaxies is well represented by the Schechter (1976) analytic form as follows

$$\phi(L)dL = \phi^* \left(\frac{L}{L^*}\right)^\alpha e^{-L/L^*} d\left(\frac{L}{L^*}\right), \quad (3)$$

where  $L^*$  is the characteristic luminosity and  $\alpha$  is the faint-end slope.  $\phi^*$  is the characteristic density, which is the normalization related to the number of luminous galaxies per unit volume (cf. Ellis 1997).

We adopt the morphology-dependent LF from the models of Roche et al. (1996, hereafter RSMF96) for our present study. For early-type galaxies, the parameters of LF assumed in RSMF96 are  $M_B^* = -21.00$ ,  $\alpha = -0.70$  and  $\phi^* = 9.68 \times 10^{-4} \text{Mpc}^{-3}$ . We derive the local LF of  $I_{F814}$  band by shifting  $M_B^*$  according to the present-day color  $B - I_{F814}$  computed by our models (see the last column

in Table 3). Note that in RSMF96, the E/S0 galaxies are divided into two types, namely, the cold and the hot ellipticals. In our case, however, we do not make such a distinction and simply incorporate them into a single type. Besides, it should be mentioned that the classification between early-type, late-type spirals and irregulars of RSMF96 LF is also suitable for future investigations, although we only deal with ellipticals in the present work. For PLE models, in contrast to the cases of number evolutions, the evolution of LF with respect to  $z$  is realized only by  $e$ -corrections (with the dust extinction involved), which are functions of  $z$ .

Considering that there exist some uncertainties in determining the local LF, as mentioned in the introduction, we attempt to vary the parameters of LF, in particular,  $\alpha$ , to show to what extent such uncertainties can affect our conclusions.

## 3 RESULTS

### 3.1 Star Formation Rates

As outlined previously, we adjust the model parameters of SFRs to fit best the observational local colors of E/S0 galaxies. The SFR is a single-parameter function taking the form of exponential decrease with respect to time, i.e.,  $\psi(t) \propto \exp(-t/\tau_e)$ , which is a natural result under the simple assumption that  $\psi(t)$  is proportional to the available gas (Kennicutt 1983), where  $\tau_e$  is the  $e$ -folding time characterizing this form of SFRs. Thus in the viewpoint of modelling, the evolutionary photometric and spectroscopic properties of galaxies can be completely determined by these parameters in our simple PLE models once the cosmological models are specified. We summarize the values of these model parameters in Table 3 in column 2 and 3. The model colors of  $U - B$ ,  $B - V$ ,  $B - R$ ,  $b_j - I$  and  $b_j - K$  are listed from column 4 to 8, for comparison with the observational ones shown in Table 2. The  $b_j - I_{F814}$  colors are also given in column 9 for converting the LF from  $b_j$  into  $I_{F814}$  band.

Table 3 shows that the modelled colors in a specific band computed by any one of our models are much close to each other, the difference from model to model is very small. The model colors are also close to the observed ones listed in Table 2. In particular, the BC97 models can reproduce better the  $b_j - K$  color than the old version (BC93) by about 0.2 – 0.3mag reddening. Considering that the uncertainties in local colors of galaxies are about 0.1 – 0.2mag, the adopted values of the parameter  $\tau_e$  should be acceptable. Furthermore, we can also find that the models can grossly reproduce the observed SEDs for E/S0 galaxies of present-day by comparing the  $k$ -corrections computed from the models with the empirical one (not shown).

Superior to the old version as it is, the BC97 models still need further refinement, especially in the UV range, for the modelled  $U - B$  colors are slightly redder than the observed one, which signals such improvements to be needed.

### 3.2 HST F814w Number Counts of Ellipticals

The wider spatial coverage of the MDS and the improved signal-to-noise of the HDF, which provide us with abundant image information, now allow us to model the morphologically segregated galaxy number counts, and we pay attention to the number counts of E/S0 galaxy in our current investigation. The observed data of elliptical galaxy number

**Table 3.**  $z_f$  and SFR parameters listed in column 2 and 3 in the three cosmological models under consideration, with the modelled colors listed from column 4 to 9.

Scenario A								
Models	$z_f$	$\tau_e^a$	$U - B$	$B - V$	$B - R$	$b_j - I$	$b_j - K$	$b_j - I_{F814}$
A1	3.5	0.8	0.64	0.92	1.67	2.27	4.10	2.03
A2	5	0.2	0.65	0.92	1.69	2.30	4.15	2.05
A3	8	1.0	0.64	0.92	1.68	2.29	4.13	2.04
A4	10	1.0	0.65	0.92	1.68	2.29	4.13	2.04
Scenario B								
Models	$z_f$	$\tau_e^a$	$U - B$	$B - V$	$B - R$	$b_j - I$	$b_j - K$	$b_j - I_{F814}$
B1	2.5	0.2	0.67	0.93	1.70	2.32	4.19	2.07
B2	3.5	0.1	0.69	0.94	1.72	2.34	4.22	2.09
B3	5	0	0.71	0.95	1.74	2.36	4.25	2.11
B4	10	1.0	0.71	0.95	1.74	2.36	4.25	2.11
Scenario C								
Models	$z_f$	$\tau_e^a$	$U - B$	$B - V$	$B - R$	$b_j - I$	$b_j - K$	$b_j - I_{F814}$
C1	2.5	0.4	0.70	0.93	1.72	2.33	4.20	2.07
C2	3.5	0.2	0.70	0.94	1.73	2.35	4.23	2.09
C3	5	0.05	0.72	0.95	1.74	2.37	4.26	2.11
C4	10	1.2	0.71	0.95	1.74	2.36	4.25	2.11

<sup>a</sup>  $\tau_e$  is the characteristic time-scale for SFRs, measured in Gyr, and  $\tau_e = 0$  represents the single burst model, in which the evolution is pure passive.

counts are taken from Glazebrook et al. (1995) and Driver et al. (1995b) for MDS, and Abraham et al. (1996) for HDF. Although there may exist some errors in the morphological classification (the scheme and details in classification have been discussed in the above-quoted works), from Figure 2 we can see that the data show gross agreement within the overlapped regions between different research group's, indicating, to some extent, that the classification is reliable. Another noteworthy feature is the flattening beyond  $I_{F814} \sim 22.5$ , which is just the unique property that is different from the counts of other types (spirals or irregulars) as well as the overall population.

Figures 2-(a), (b) and (c) show differential number counts derived from the F814w bandpass on board HST, together with our models in the three scenarios A, B and C indicated by lines. Apparently, the non-evolutionary predictions cannot reproduce the data, either at faint magnitudes or at the bright end. The predictions with luminosity evolution, however, can match better the number counts at bright end up to  $I_{F814} \sim 21.0$ mag, no matter which scenario, and which  $z_f$  in each scenario is taken into account, i.e., the number counts at bright magnitudes are insensitive to geometry or  $z_f$ . The effect of luminosity evolution is significant and should not be neglected. Furthermore, allowing for the fluctuation of the Glazebrook et al. sample at bright magnitudes, we believe that the normalization of the RSMF96 LF employed in this work is reasonably well.

Discrepancies between these evolutionary predictions do exist and occur beyond  $I_{F814} > 21.0$ mag. We will discuss them in detail the the following.

### 3.2.1 Scenario A

All the predictions fall within the error bars of the data, while only the model of  $z_f = 5$  predicts better the number count than the others. Besides, it can grossly reproduce the faint-end flattening at around  $I_{F814} \sim 23.0 - 25.0$ . For the case of  $z_f = 3.5$ , though it keeps on increasing up to  $\sim 23.0$ mag and reproduces better the counts even than that of  $z_f = 5$  model at  $I_{F814} \sim 21.0 - 23.0$ , it will turnover consequently and greatly underpredict the faint-end counts as well as the flattening. It seems that  $z_f = 3.5$  for a flat Einstein-de Sitter world model is not proper, since it is too low, and hence there is not enough volume to accommodate sufficient objects. While if the  $z_f$  is chosen as high as 8 or 10, the models will predict much lower counts from  $I_{F814}=20.5$  to 22.5 than the others.

### 3.2.2 Scenario B and C

Models of  $z_f = 10$  can be absolutely ruled out: the predictions at  $I_{F814} > 24.0$  overshoot the HDF data by about a factor of 3 to 4, indicating that volumes in the two world models at such a redshift are both too large; they simultaneously underpredict the counts at  $I_{F814} = 21.0 - 24.0$  mag (Scenario B) or 21.0 - 23.0 mag (scenario C), indicating that luminosity evolutions in the two cases are both too low.

The prediction seems better for  $z_f = 2.5$  in Scenario B, since it can reproduce well the counts almost at every magnitude from 21.0 to 25.0 mag. It is also not bad for Scenario C, though the prediction at 23.0 - 24.0 mag is slightly higher than that of Scenario B.

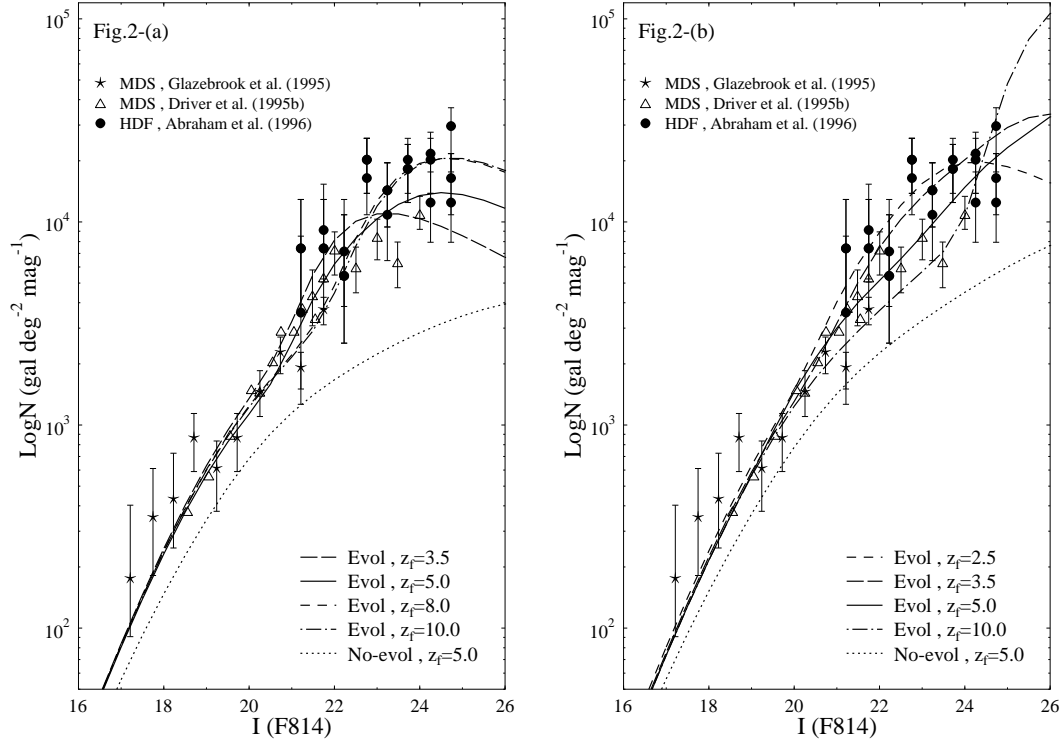
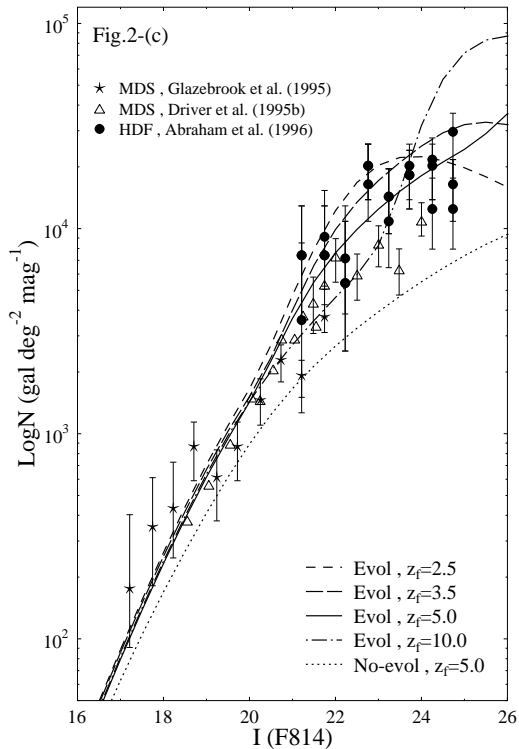


**Figure 2.** The differential number counts for E/S0 galaxies as a function of apparent magnitude in  $I_{F814}$  band. Figures 2-(a), (b) and (c) are for Scenario A, B, and C, respectively. The sources of the observational data are exhibited in the figure and these data are indicated by symbols. The models are shown by lines.



The predictions are not as good as those of  $z_f = 2.5$  for models of  $z_f = 5.0$  in either Scenario B or C. In particular, the slopes  $\gamma \equiv d \log N(m)/dm$  of the models at  $I_{F814} > 22.5$

mag are  $\sim 0.22$  and  $\sim 0.18$  for Scenario B and C, respectively, steeper than the flattening of the observational data. It, however, should be attributed not to the evolution but to the geometry, since the evolution is nearly passive (see Table 3). As can be seen, the slopes even for non-evolutionary models are still as high as  $\sim 0.12$  and  $\sim 0.14$  for Scenario B and C, respectively. Regardless of the steep slopes, there is neither sufficient nor convinced evidence to exclude such models as  $z_f = 5.0$ . After all, our models reproduce the counts within the magnitude range where there exist observational data ( $I_{F814} = 17.5 - 25.0$  mag).

The  $z_f = 3.5$  models of Scenario B and C can be regarded as interpolations between the models for  $z_f = 2.5$  and  $z_f = 5$ , but they are more similar to those of  $z_f = 5$ .

### 3.3 Redshift Distribution

In modern astronomy, redshift distributions of galaxies are the key measurement required to probe the local luminosity function, or possible evolution taking place in galaxies as well as the geometry of the universe. Such measurement has already reached up-to-date as faint as  $B \sim 24$  mag by the new spectroscopic samples derived from the Keck Telescope (Cowie et al. 1995, 1996). It can be seen from Section 3.2, that the conclusions are rather uncertain and obscure. Hence, we should incorporate redshift distributions for bins of observed magnitudes, to continue our investigation. Such exploration will be conducive to the understanding of our models, though such spectroscopic data has not been obtained morphologically as yet.

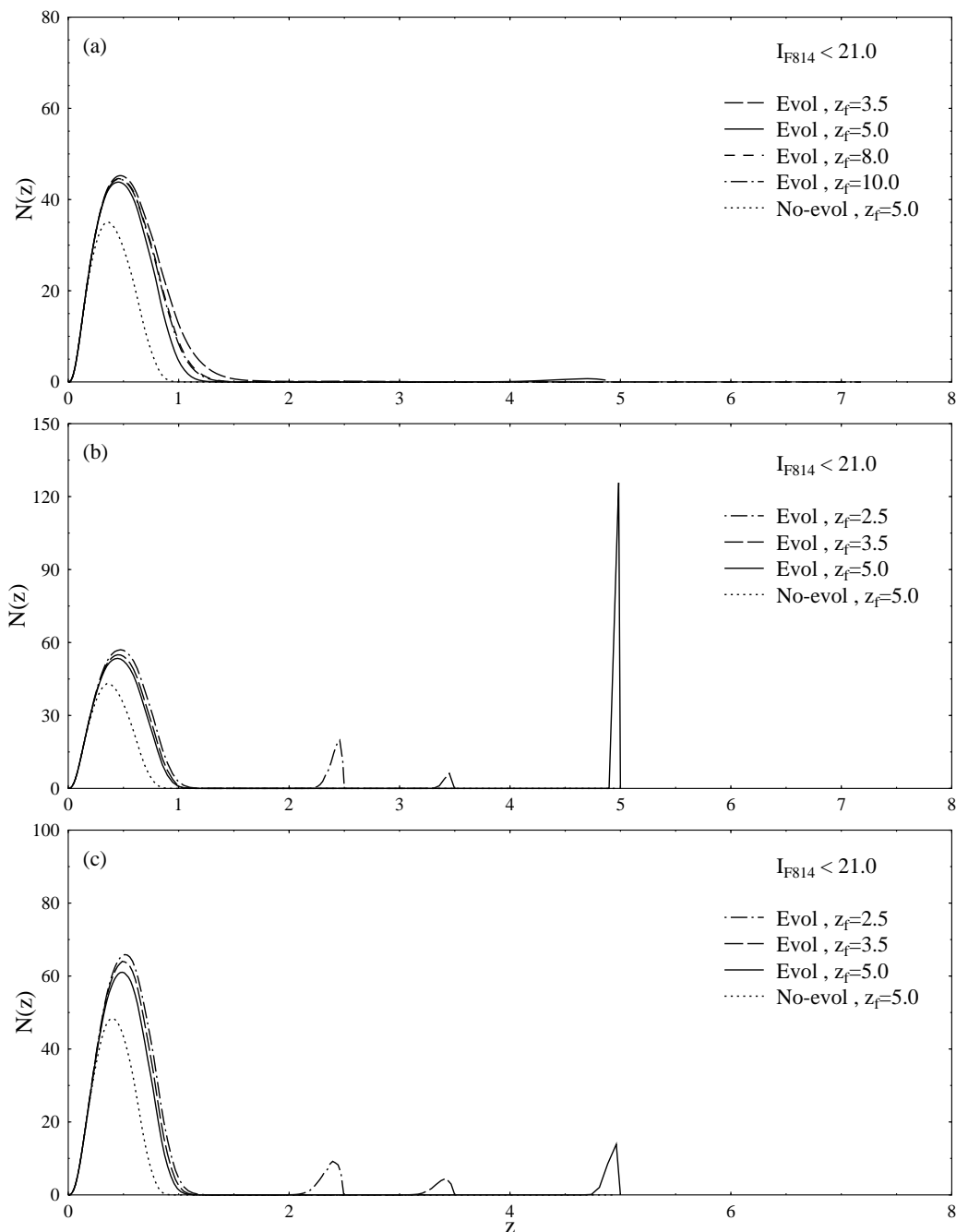


**Figure 3.** The  $z$ -distribution of  $F814w < 21.0$ . Panels (a), (b) and c are for Scenario A, B and C respectively. Models are indicated by lines. The model predictions have been normalized in the unit of  $\text{deg}^{-2}$  with redshift bin  $\Delta z = 0.01$ .

### 3.3.1 $z$ - distribution of $I_{F814}$ -band

#### (a) $I_{F814} < 21.0$

In Figure 3 we plot our predictions for the redshift distributions of  $I_{F814} < 21.0$  mag. Panels (a), (b) and c are for Scenario A, B and C, respectively. We re-scale our predictions in the unit of  $\text{deg}^{-2}$  with redshift bin  $\Delta z = 0.01$ . We can see that all the models with evolution will peak at  $z \sim 0.5$  (hereafter, we call it the first), but it can also be seen that there is another peak existing at the redshift of  $z_f$  (hereafter, we call it the second), except for Scenario A. In particular,

the second peak of  $z_f = 5.0$  model in Scenario B is more than two times as high as the first. An extremely rapid declining of the SFR (for the  $z_f = 5.0$  model in Scenario B, the time scale  $\tau_e = 0$ , i.e., single burst) will consume (almost) all the gas in galaxies to form stars (almost) in an instantaneous burst, rendering the galaxies to be detectable at that high redshift, not bringing about the subsequent star formation, especially of massive stars, and resulting in the rapid fading in luminosity of galaxies shortly after the formation of stars of the first generation. Therefore, the existence of the second peak should be completely attributed to the rapid lu-

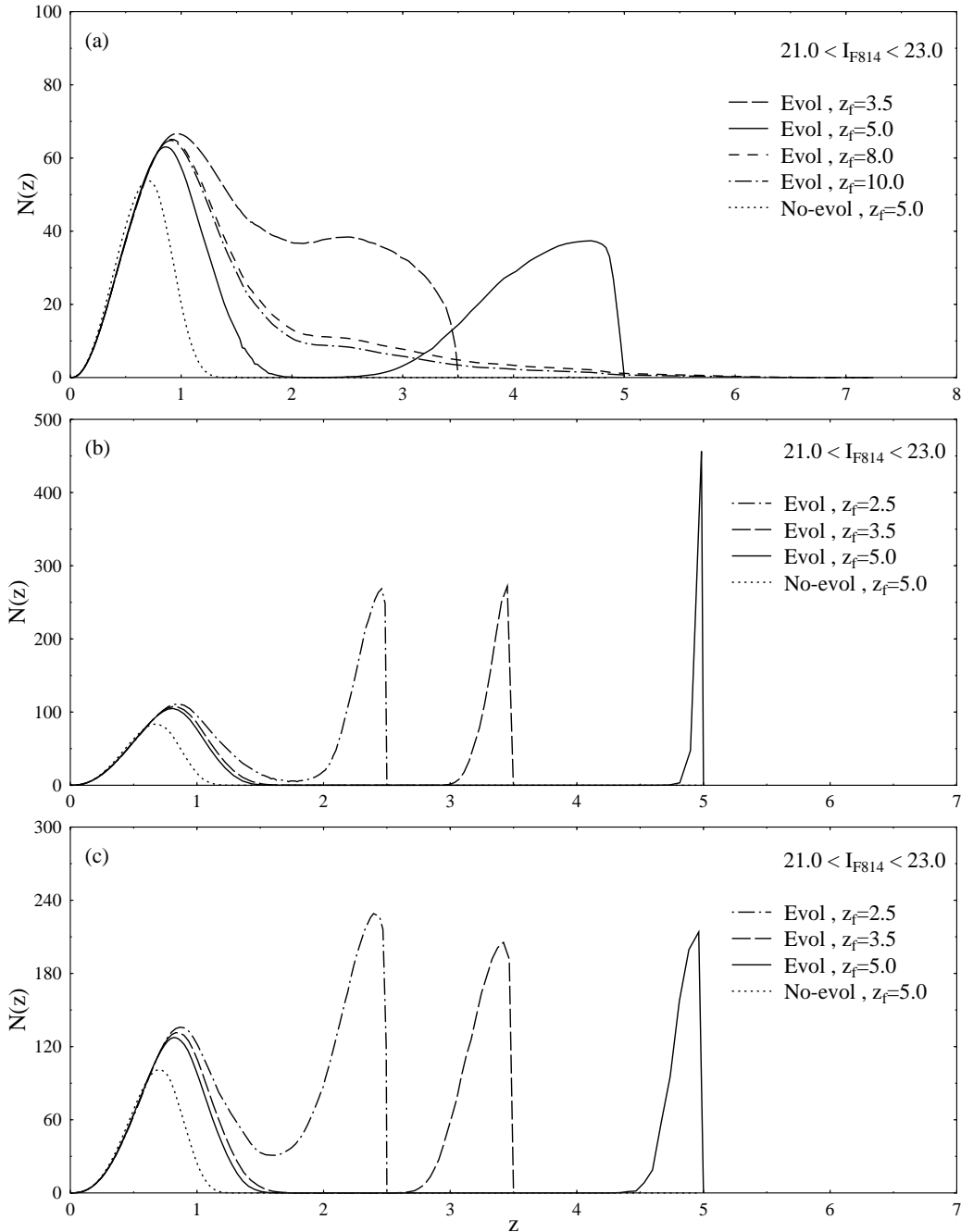


**Figure 4.** The  $z$ -distribution of  $21.0 < I_{F814} < 23.0$ . Panels (a), (b) and c are for Scenario A, B and C respectively. Models are indicated by lines. The normalization is the same as Figure 3.

minosity evolution. Yet the peak is very narrow, and hence it will not be expected to contribute too much to the counts.

(b)  $21.0 < I_{F814} < 23.0$

Figure 4 is plotted for the predictions of the redshift distribution limited in  $21.0 < I_{F814} < 23.0$ , the others are the same as Figure 3. For Scenario B and C, it can be seen that the high- $z$  peaks of the  $z_f = 5.0$  models are even higher than those in the case of  $I_{F814} < 21.0$ , but the contributions to the counts are still not comparable to the first. As for Scenario A, it is obvious that the high- $z$  contribution begins

to be significant for the models whose  $z_f = 3.5$  or  $5.0$ . What forms the sharp contrast is that there are no such peaks in the predictions of the  $z_f = 8.0$  or  $10.0$  models. It is just the absence of these peaks that leads to the lower number counts at around  $I_{F814} \sim 20.5$  to  $\sim 22.5$  mag than those of  $z_f = 3.5$  or  $5.0$  models (see Figure 2-(a)).

(c)  $23.0 < I_{F814} < 25.0$

Figure 5 is for the redshift distributions predicted by our models within the magnitude range  $23.0 < I_{F814} < 25.0$ . All the curves of the models are similar to those in the case



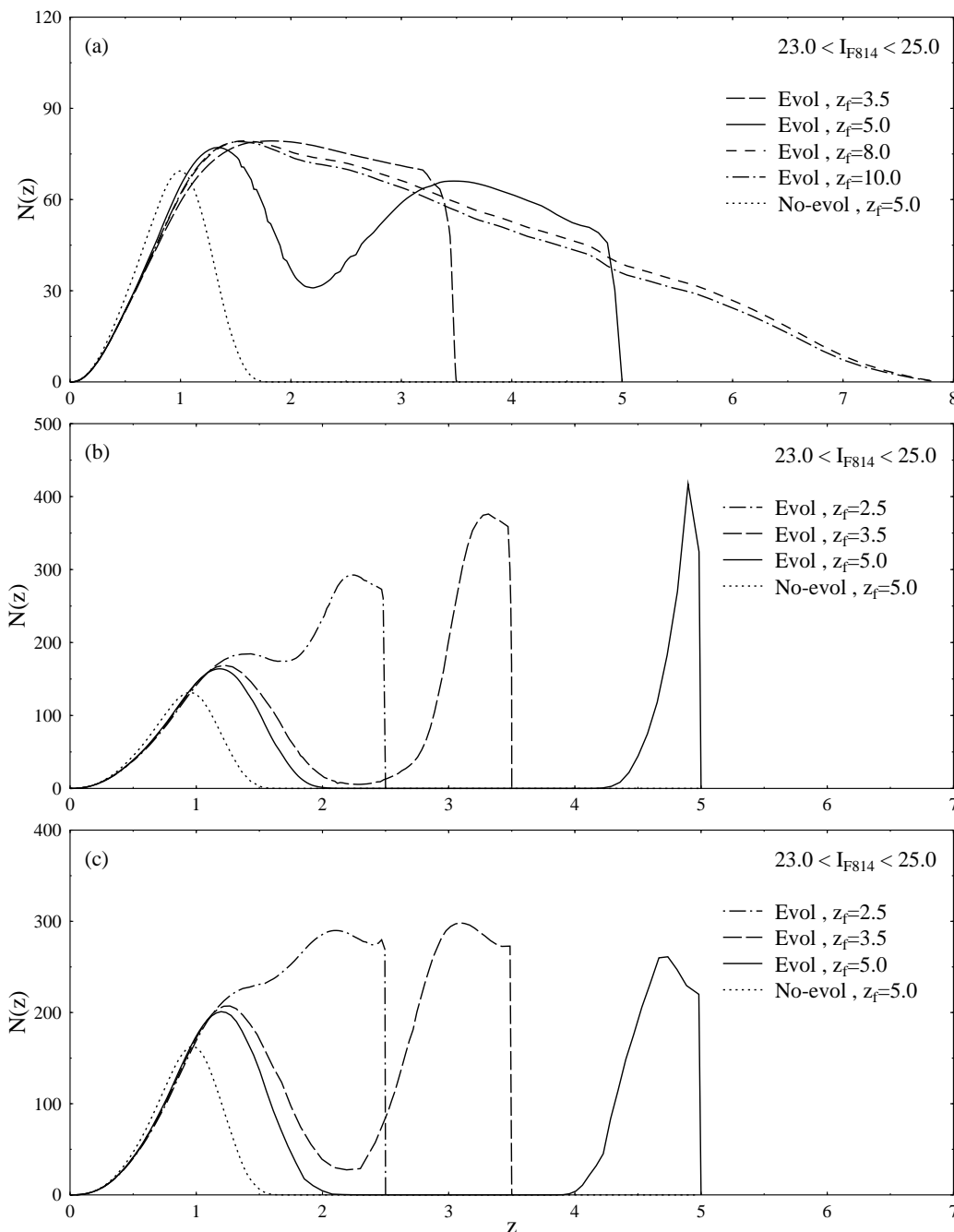


**Figure 5.** The  $z$ -distribution of  $23.0 < F814w < 25.0$ . Panels (a), (b) and c are for Scenario A, B and C respectively. Models are indicated by lines. The normalization is the same as Figure 3 and Figure 4.

of  $21.0 < I_{F814} < 23.0$ , except that high- $z$  contributions become dominant in such faint magnitude range, especially for Scenario A, as can be seen from the figure.

In each of the three figures above-mentioned, we have also plotted predictions of non-evolutionary models of  $z_f = 5.0$  for each panel to make comparison with the evolutionary predictions. The most significant difference between the non- and the evolutionary models can be seen from these figures is that no high- $z$  peaks appear in the predictions of non-evolutionary models. Hence, according to the PLE models, and differing from nE ones, the objects at high- $z$

also contribute to the predicted number counts at magnitudes fainter than  $I_{F814} \sim 20.5$ . Our PLE models presented here are characterized by these high- $z$  peaks in the predictions of redshift distributions.

It is worthwhile to mention that these peaks, in principle, are detectable through the F814w band-pass since  $z_L$  for F814w is  $\sim 7.8$ , which is larger than the redshift at which these peaks are seen.

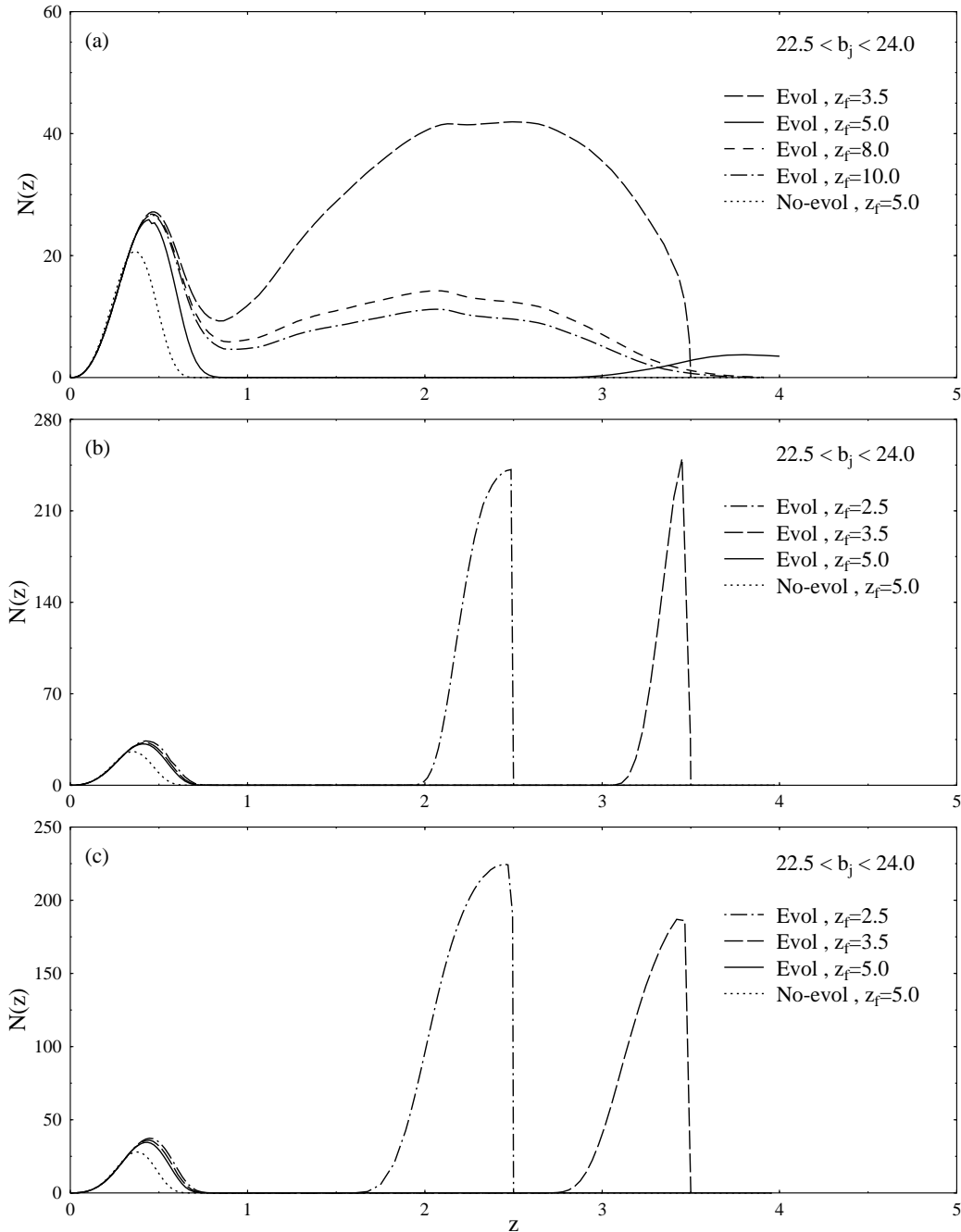


**Figure 6.** The  $z$ -distribution of  $22.5 < b_j < 24.0$ . Panels (a), (b) and (c) are for Scenario A, B and C respectively. Models are indicated by lines. The normalization is the same as Figure 3 to Figure 5.

### 3.3.2 $z$ - distribution of $22.5 < b_j < 24.0$

Since there are both abundant and deep enough spectroscopic samples in  $B$ -band surveys up to date, the predictions of  $z$  distributions in this passband is of great significance. In Figure 6, we present the predicted  $z$  distributions by our PLE models within the magnitude range  $22.5 < b_j < 24.0$ . From panels (a), (b) and (c) we can see that: 1) The high- $z$  peaks for  $z_f = 5.0$  models are absent in all of the three cosmological models adopted currently. The shapes of these curves are similar to those of non-evolutionary ones, except

that for Scenario A, where there is merely a little rise beyond  $z=3$ , and 2) the high- $z$  peaks or tails still exist in  $z_f=2.5$  or  $3.5$  models in any scenario. As mentioned in Section 2, the light coming from beyond  $z_L$  will be greatly reduced by Lyman absorption, hence the objects beyond  $z_L$  are hardly detectable, and that  $z_f > 4.0$  (for  $b$ -band,  $z_L = 4.0$ ) is favoured by the  $z$  distribution of  $22.5 < b_j < 24.0$  in any world models. On the contrary,  $z_f=2.5$  or  $3.5$  are not appropriate choices, unless the high- $z$  tail or the high- $z$  peak can be detected in the future.

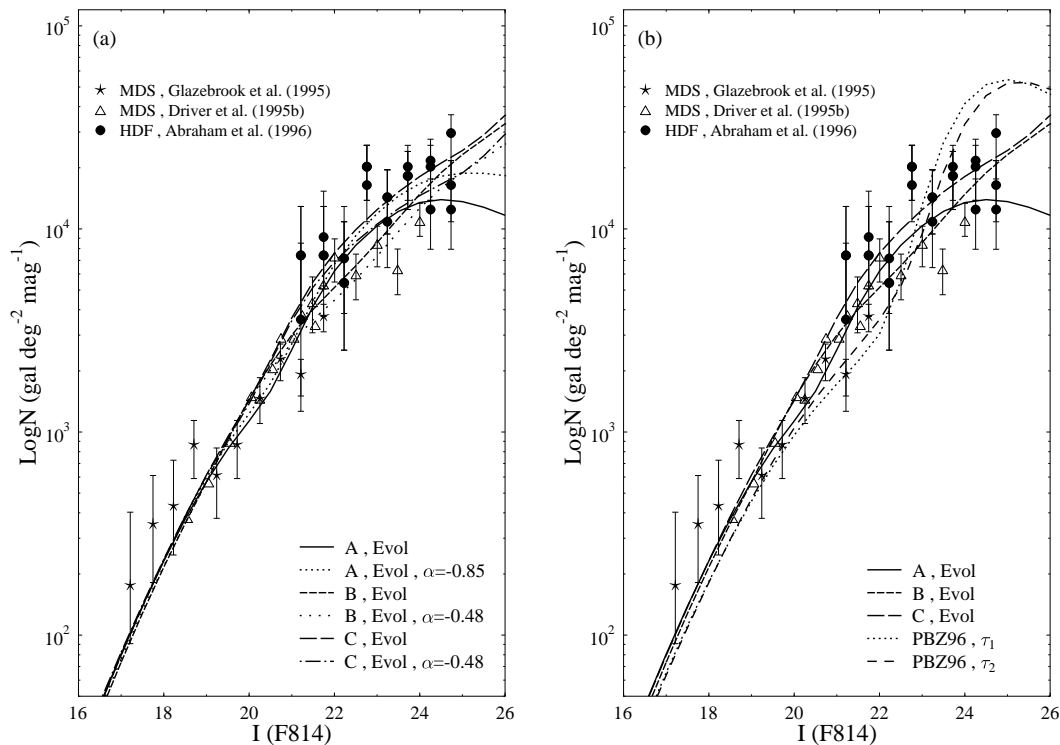


**Figure 7.** The differential number counts for E/S0 galaxies as a function of apparent magnitude in  $I_{F814}$  band. The models are for  $z_f = 5.0$ , which are shown by lines. The letter A, B and C in the figure represent Scenario A, B and C, respectively. Panel (a): Comparison with the results of varying the faint-end slope of LF; (b): Comparison with the results of PBZ96.

## 4 DISCUSSION

### 4.1 Uncertainties in LF

As mentioned in Introduction, there may exist many uncertainties in determining the local LF, hence there is no reason in believing that the LF in our present work is the unique adoption. We will explore the influence of the uncertainties in LF upon our conclusions, in particular, upon the number counts, simply by varying the LF parameters. From the previous investigation, we have already seen that the normalization, which involves both  $\phi^*$  and  $M^*$  (cf. Ellis 1997), is appropriate. Thus we only concentrate on the faint-end slope  $\alpha$ . The following concerns only the  $z_f=5.0$  models.

For Scenario A, we choose a higher value for  $\alpha$ , say,  $-0.85$ , which is slightly lower than  $-0.9$ , the value of Marzke et al. (1994a, 1994b). For Scenario B and C, we adopt  $-0.48$ , the value of PBZ96. From Figure 7-(a) we can see that such variation will not affect the counts at bright magnitudes, and will not bring about too much change at the faint-end, either. For Scenario A, such variation leads to only  $0.12\text{dex}$  higher than that of  $\alpha = -0.70$  at  $I_{F814} = 25.0$ . But the faint-end slope of the number-count curve  $\gamma$  is better than its counterpart of  $\alpha = -0.70$ . As for Scenario B and C, such variation does not make too much difference. Hence, through such prescriptions, we have verified that the *uncertainties* in LF (will) not influence too much our conclusions.

### 4.2 Comparison with Other Works

We notice that the PLE model by PBZ96, which was constructed under the BC93 spectral evolution models in a

world model with  $\Omega \sim 0$ , can account for most of the observed photometric and spectroscopic properties of galaxies, including the number counts in the  $U, b_j, r_f, I$  and  $K$  bands, as well as the color and redshift distributions derived from most of the existing samples. We have interest in examining whether the parameters of the PBZ96 model adopted for E/S0 are suitable for the modelling of early-type galaxy number counts in the  $I_{F814}$  passband. The  $e+k$ -correction for E/S0 galaxies in  $I_{F814}$  band is computed by employing BC93 models, exactly in terms of the parameters adopted by PBZ96. From Figure 7-(b), we can see that, compared with our models, neither the  $\tau_1$  nor the  $\tau_2$  model of PBZ96 (Following PBZ96,  $\tau_1$  and  $\tau_2$  refer to the time scale of SFR  $\tau_e$  being 1Gyr and 2Gyr, respectively, with IMF adopted as Scalo one for ellipticals.) can reproduce the number counts of E/S0 galaxies properly. Furthermore, the adoption of a  $\Omega \sim 0$  cosmological model is obviously unphysical.

As can be seen from Section 3.2, our PLE models can reproduce the number counts well in all three cosmological models under consideration, especially for Scenario C (the world model dominated by a  $\lambda$ ), as seems to be conflicting with the result of Driver et al. (1996), who concluded that flat models dominated by a cosmological constant are ruled out from comparison of their E/S0 counts (Driver et al. 1995b) with their model predictions. The difference between our models and Driver et al.'s (1996) lies in the normalization of E/S0 galaxy counts, i.e., a much higher normalization adopted by Driver et al. Besides, the E/S0 counts for MDS of Driver et al. are apparently lower than the HDF counts of Abraham et al. (1996).

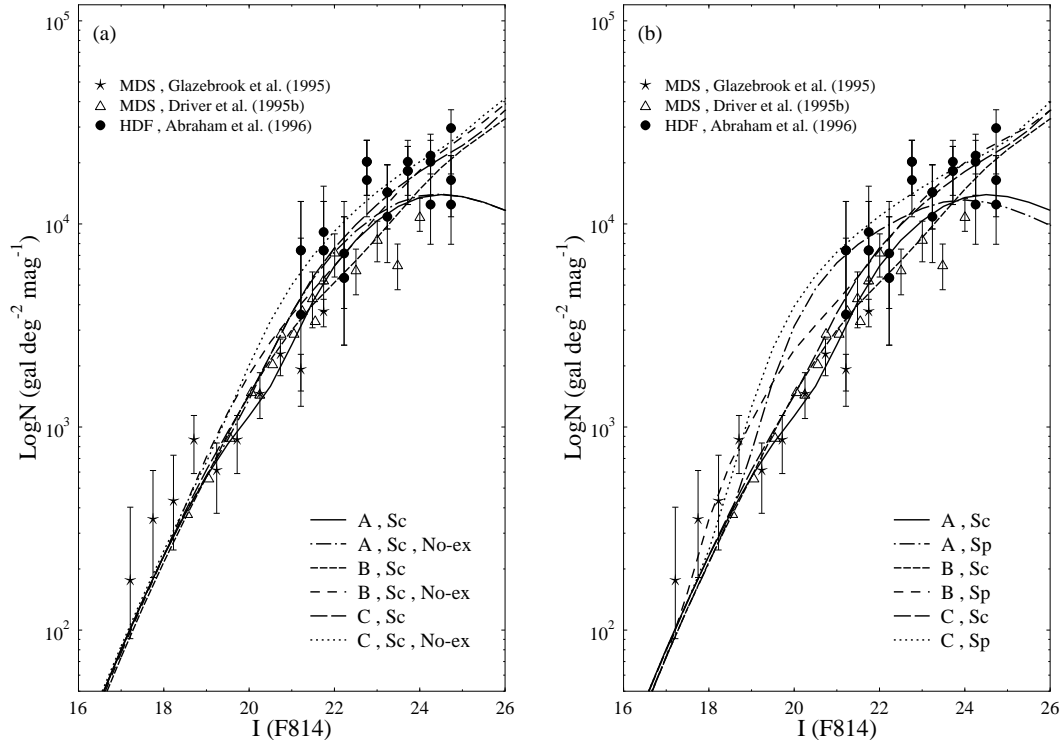


**Figure 8.** The differential number counts for E/S0 galaxies as a function of apparent magnitude in  $I_{F814}$  band. The models are for  $z_f = 5.0$ , which are shown by lines. In the two panels, the symbols ‘Sc’ and ‘Sp’ denote Scalo and Salpeter IMF, respectively. ‘No-ex’ means no dust extinction is involved. Panel (a): Comparison with the results of no dust extinction; (b): Comparison with the results by assuming Salpeter IMF.

### 4.3 Dust extinction and IMF

We have taken into account to some extent the influence of dust extinction on the predictions of the models, as described in Section 2.3. From Figure 8-(a), we can see that the effect of dust extinction is obvious, especially for Scenario B and C, such that models without extinction will predict more ellipticals than observed from  $I_{814} \sim 19$  to  $\sim 21$ . Moreover, the high- $z$  tails or peaks are even higher than the results if dust is not considered in the models (see Figure 9).

The Scalo IMF is more favoured by the observations than the Salpeter IMF. It can be seen from Figure 8-(b), even with dust extinction involved, the models can not reproduce satisfactorily the number counts, and greatly overestimate the counts between  $I_{814} \sim 19 - 21$ . A less steep IMF at high-mass end such as the Salpeter one will lead to more massive stars existing at early times, rendering UV fluxes are so strong that more galaxies can be detected at high- $z$  (see Figure 9).

## 5 SUMMARY AND CONCLUSIONS

We believe that in any realistic evolutionary models, the luminosity evolution must be considered, since there exists a well-known fact that galaxies are composed of stars, and stars continuously come into birth and evolve into the post-main-sequence. The lifetime of stars depends on their mass. This leads to the continuous change of the photometric and spectroscopic properties of galaxies. Although nE models

can work sometimes (Driver & Windhorst 1995a), it is obviously unphysical and can only be treated as baseline for comparison with observations and other models. In this paper, we have constructed a series of PLE models in the three cosmological models to explain the observed number counts for elliptical galaxies in MDS and HDF obtained by the HST. We summarize our investigations in the following.

i) Although some of our model colors do not match quite well the observed ones, for example, in all cases, the  $U - B$  color is slightly redder than the observed, the success of the BC97 population synthesis model which our present work is based upon is still worthy of being affirmed. More recently, Steidel et al. (1996) found that high-redshift galaxies are also well described by the (BC93) models. It should be pointed out that some complexities are neglected in the current prescription of simple PLE models, e.g., we have not modelled the evolution of metallicity in our work. There exists, however, a so-called *age-metallicity degeneracy* stating that for stellar populations older than 2Gyr, an increase in metallicity by a factor of 2 and a decrease in age by a factor of 3 results in almost identical optical and near-IR colors (Worthey 1994). Therefore, when a formation redshift  $z_f$  is assumed so that the age of galaxies is determined in a specific cosmological model, the effect of evolution of metallicity can be partly compensated by the appropriate adoption of the parameters of SFR  $\tau_e$ . This will also from the other side indicate that the local colors are insensitive to the adoption of  $z_f$ , as can also be seen from Table 3.

ii) The Hubble constant  $H_0$  plays just a minor role in

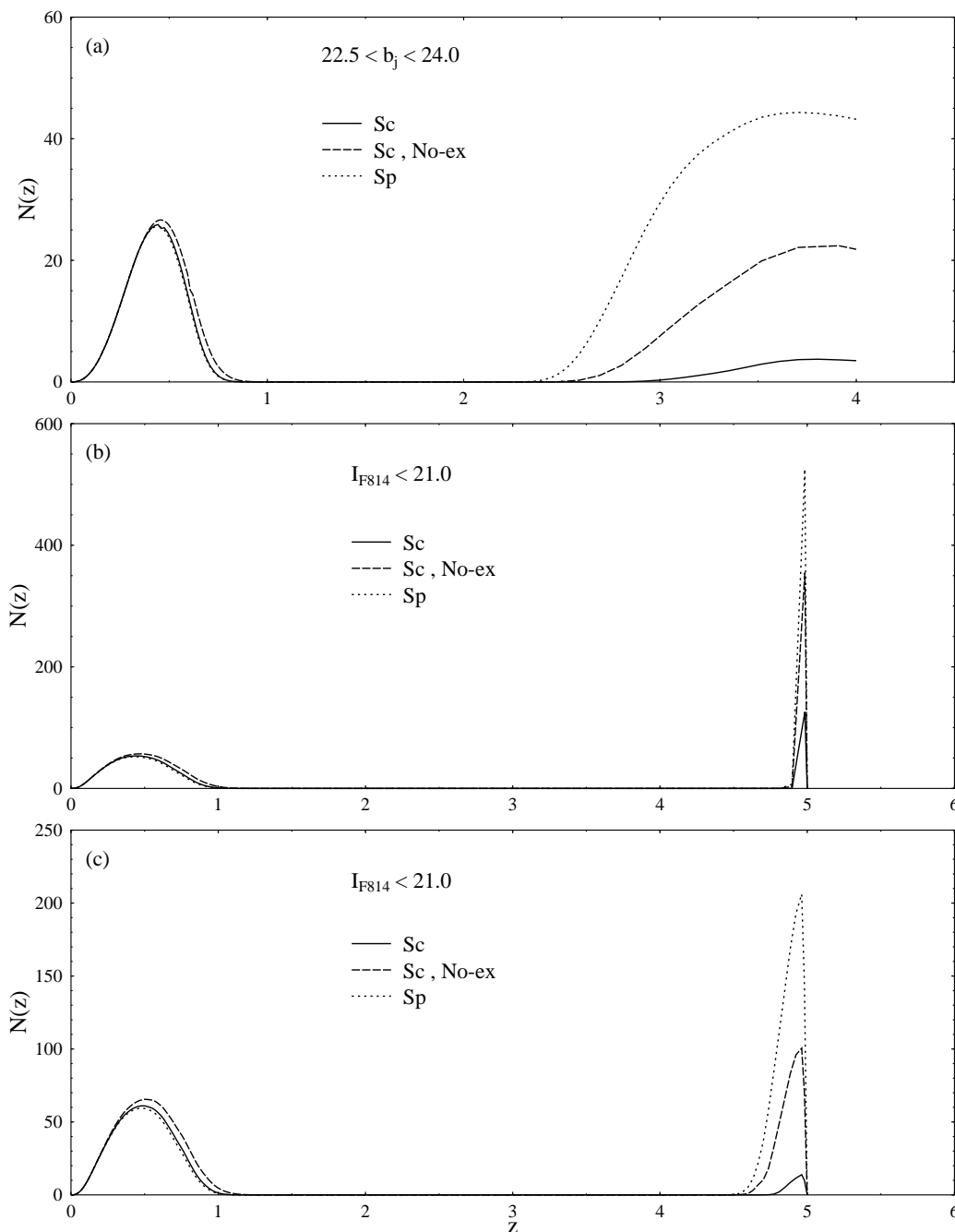


**Figure 9.** The  $z$ -distribution for ellipticals. Models are indicated by lines. Meanings of the symbols are the same as those in Figure 8. Panel (a) is for Scenario A, limited in  $22.5 < b_j < 24.0$ ; panels (b) and (c) are for Scenario B and C respectively, limited in  $I_{F814} < 21.0$ .

our present investigation. Although  $H_0$  is included in the normalization  $\phi^*$  and characteristic luminosity  $L^*$  of LF, it can be canceled out by the quantities relative to cosmology. The only aspect needed to pay attention to is that the age of galaxies is measured in  $H_0^{-1}$ . Hence the age of galaxies will be smaller if a larger  $H_0$  is adopted, and vice versa, as will more or less influence the modelled spectra of galaxies. The adoption of  $H_0 = 50 \text{ km s}^{-1} \text{ Mpc}^{-1}$  seems quite reasonable for a flat world model with  $\Omega = 1$ . We can see from Table 3 that the integrated colors computed by the latest BC97 spectral evolutionary models are appropriate com-

pared with the observed locally (Table 2). Hence regardless of the  $H_0$ /globular cluster age problem, the flat cosmological model will not suffer from the conflict of color/age in the context of BC97 models.

iii) In spite of the fact that the models of  $z_f = 5.0$  failed to predict the faint-end flattening of the number counts in Scenario B or C, our PLE models can still be regarded to have reproduced well the data from the MDS and the HDF up to  $I_{F814} \sim 25$  within the range of uncertainties in all the three scenarios. The corresponding predicted  $z$ -distribution of  $22.5 < b_j < 24.0$ , though we have not observed data to

compare with, does not present a high- $z$  tail or peak. The shapes of evolutionary predictions are similar to those of no-evolution for the  $z$  distribution, with the mean redshift  $z_m$  slightly higher than the no-evolution's, as can be attributed to the effect of luminosity evolution.

iv) The above conclusions are not affected by the variation of the LF parameters ( $\phi^*$ ,  $\alpha$  and  $L^*$ ). Hence, even though there may exist some uncertainties and biases in the determination of local LF, the above conclusions are still valid and reliable.

v) The law of dust extinction for ellipticals is largely uncertain. We simply extrapolate the Wang's approach to the current case, and the results seem to be well in agreement with the observed extinction in  $B$  band for present-day ellipticals. By such an *ad hoc* assumption, together with the adoption of Scalo IMF for ellipticals, UV fluxes can be greatly reduced at high redshifts, leading to the high- $z$  peaks substantially depressed. Moreover, the predictions of number counts are also improved.

vi) High  $z_f$ , say 5.0, and nearly-passive evolution shortly after a (nearly) single burst to form most of the stars (in our work,  $\tau_e=0.2$ , 0 and 0.05Gyr for Scenario A, B and C, respectively) are critical for the modelling, as is just the case of the conventional scenario for formation and evolution of ellipticals (cf. Eggen, Lynden-Bell & Sandage 1962; Partridge & Peebles 1967). On the contrary, it will not be favoured by, especially, spectroscopic samples that galaxies formed at as low as  $z_f = 2.5$  (or 3.5), or the evolution is as large as that of PBZ96, unless more exotic scenarios are introduced into the modelling.

vii) We do not touch upon the possibilities of number evolutions in the present investigation, though it has been widely considered to account for the optical/infrared and the photometric/spectroscopic paradox (see Introduction). Even though there may be the possibility that a new population of dwarf galaxies existed at high- $z$  and then faded or disappeared lately, it is unlikely that they are of early-type galaxies, or at least most of them can not be early-types. If so, the faint-end slope of number counts of early-type galaxies will be steeper than the currently observed data from HST. The assumption of mergers is also not necessary here, though the possibility of mergers is not ruled out. If the scenario of merging is taken into account, a series of problems will be involved (cf. Tóth Ostriker 1992; Babul & Ferguson 1996, and references therein), and the physical mechanism for mergers is much more complicated than that of PLE.

viii) We have chosen three cosmological models for our work. The predictions of number counts by the flat Einstein-de Sitter model agree well with the observed data, so do the open Friedmann-Robertson-Walker model ( $\Omega_0=0.1$ ,  $\lambda_0=0$ ,  $H_0=50 \text{ km s}^{-1} \text{ Mpc}^{-1}$ ) and the Friedmann-Lemaître model ( $\Omega_0=0.2$ ,  $\lambda_0=0.8$ ,  $H_0=60 \text{ km s}^{-1} \text{ Mpc}^{-1}$ ). Therefore, we can not discriminate between these cosmological models by the galaxy number counts. Our conclusion here contradicts with that of Driver et al. (1996), who announced that the world models dominated by a  $\lambda$  are ruled out by their modelling of E/S0 number counts. Like many other authors (Tinsley 1972; Ellis 1997), we believe that the formation and evolution of galaxies is a problem far from being well understood, and any definite judgment about world models, whether the universe is open, flat, closed or  $\Lambda$ -dominated, can not be made as yet by the number counts.

ix) As mentioned previously, our PLE models do not include the evolution of metallicity with respect to  $z$ , and those details such as the recycling of the residual gas ejected by the dying stars as well as some selection effects are also ignored in our models. These can be considered as further improvement over our present models.

All in all, the models presented in this work can explain well the number counts of elliptical and S0 galaxies derived from HST under the assumption of PLE. It is unlikely that the problem of FBGs is caused by early-type galaxies, and we hold identical views as other researchers (Driver & Windhorst 1995; Driver et al. 1995; Glazebrook et al. 1995; Abraham et al. 1996) on this. Furthermore, our work shows that the cosmological parameters can not be determined by up-to-date observations. In a forthcoming paper, we will devote ourselves to the galaxy number counts of the other morphological types segregated by HST, namely, the early-type spirals (Sabc) and late-type spirals and irregulars (Sdm/Irr), as well as the overall populations, with the present results and conclusions involved, which will be examined further.

## ACKNOWLEDGMENTS

P. He should like to thank Mr. S. Charlot for providing us with their synthesis spectral evolutionary models and helpful correspondences. We acknowledge the valuable discussion between Dr. B.F. Roukema, Prof. Z.G. Deng and Prof. Z.L. Zou. The authors are much grateful to Mrs. B. Poggianti for her constructive comments and suggestions to improve the manuscript of this paper. We also thank The State Key Laboratory of Science and Engineering Computing (LSEC) of Academia Sinica for providing us with computer supports. This work is in part supported by the National Natural Science Foundation of China.

## REFERENCES

- Abraham R. G., Tanvir N. R., Santiago B. X., Ellis R. S., Glazebrook K., van den Bergh S., 1996, MNRAS, 279, L47
- Babul A., Rees M. J., 1992, MNRAS, 255, 346
- Babul A., Ferguson H. C., 1996, ApJ, 458, 100
- Broadhurst T. J., Ellis R. S., Shanks T., 1988, MNRAS, 235, 827
- Broadhurst T. J., Ellis R. S., Glazebrook K., 1992, Nat, 355, 55
- Brown G. S., Tinsly B. M., 1974, ApJ, 194, 555
- Bruzual A. G., Kron R. G., 1980, ApJ, 241, 25
- Bruzual A. G., Charlot S., 1993, ApJ, 405, 538 (BC93)
- Bruzual A. G., Charlot S., 1997, in preparation (BC97)
- Campos A., Shanks T., 1995, astro-ph/9511110, preprint 23 Nov 1995
- Carlberg R. G., Charlot S., 1992, ApJ, 397, 5
- Charlot S., Bruzual A. G., 1991, ApJ, 367, 126
- Colles M., Ellis R. S., Taylor K., Hook R. N., 1990, MNRAS, 244, 408
- Colles M., Ellis R. S., Broadhurst T. J., Taylor K., Bruce A., 1993, MNRAS, 261, 19
- Couch W. J., Newell E. B., 1980, PASP, 92, 746
- Cowie L. L., Gardner J. P., Lilly S. J., McLean I., 1990, ApJ, 360, L1
- Cowie L. L., Songaila A., Hu E. M., 1991, Nat, 354, 460
- Cowie L. L., 1991, Phys. Scripta, T36, 102
- Cowie L. L., Hu E. M., Songaila A., 1995, Nat, 377, 603

Cowie L. L., Songaila A., Hu E. M., Cohen J. G., 1996, *AJ*, 112, 839  
 De Propriis R., Pritchett C. J., Harris W. E., McClure R. D., 1995, *ApJ*, 450, 534  
 Disney M. J., 1976, *Nat*, 263, 573  
 Draine B. T., Lee H. M., 1984, *ApJ*, 285, 89  
 Driver S. P., Windhorst R. A., 1995a, astro-ph/9511134, preprint 28 Nov 1995  
 Driver S. P., Windhorst R. A., Ostrander E. J., Keel W. C., Griffiths R. E., Ratnatunga K. U., 1995b, *ApJ*, 449, L23  
 Driver S. P., Windhorst R. A., Phillipps S. and Bristow P. D., 1996, *ApJ*, 461, 525  
 Eggen O. J., Lynden-Bell D., Sandage A. R., 1962, *ApJ*, 136, 748  
 Ellis R. S., 1997, *ARA&A*, 35, 389  
 Ferguson H., McGaugh S. S., 1995, *ApJ*, 440, 470  
 Fukugita M., Takahara F., Yamashita K., Yoshii Y., 1990, *ApJ*, 361, L1  
 Fukugita M., Shimasaku K., Ikhikawa T., 1995, *PASP*, 107, 945  
 Gardner J. P., Cowie L. L., Wainscoat R. J., 1994, *ApJ*, 415, L9  
 Glazebrook K., Ellis R. S., Santiago B., Griffiths R., 1995, *MNRAS*, 275, L19  
 Goudfrooij P., 1996, astro-ph/9601169, preprint 30 Jan 1996  
 Gronwall C., Koo D.C., 1995, *ApJ*, 440, L1  
 Guiderdoni B., Rocca-Volmerange B., 1987, *A&A*, 186, 1  
 Guiderdoni B., Rocca-Volmerange B., 1990, *A&A*, 227, 362  
 Guiderdoni B., Rocca-Volmerange B., 1991, *A&A*, 252, 435  
 Hubble E. P., 1926, *ApJ*, 64, 321  
 Im M., Casertano S., Griffiths R. E., Ratnatunga K. U., Tyson J. A., 1995, *ApJ*, 441, 494  
 Johnson H. L., Morgan W. W., 1953, *ApJ*, 117, 313  
 Kauffmann G., Guiderdoni B., White S. D. M., 1994, *MNRAS*, 267, 981  
 Kennicutt R. C., 1983, *ApJ*, 272, 54  
 King C. R., Ellis R. S., 1985, *ApJ*, 288, 456  
 Koo D. C., Kron R. G., 1992, *ARA&A*, 30, 613  
 Lidman C. E., Peterson B. A., 1996, *MNRAS*, 279, 1357  
 Loveday J., Peterson B. A., Efstathiou G., Maddox S. J., 1992, *ApJ*, 390, 338  
 Madau P., 1995, *ApJ*, 441, 18  
 Maddox S. J., Sutherland W. J., Efstathiou G., Loveday J., Peterson B.A, 1990a, *MNRAS*, 247, 1p  
 Maddox S. J. et al., 1990b, *MNRAS*, 243, 692  
 Marzke R. O., Geller M. J., Huchra J. P., Corwin Jr H. G., 1994a, *AJ*, 108, 437  
 Marzke R. O., Huchra J. P., Geller M. J., 1994b, *ApJ*, 428, 43  
 Metcalfe N., Fong R., Shanks T., 1995, *MNRAS*, 274, 769  
 Metcalfe N., Shanks T., Fong R., Roche N., 1995, *MNRAS*, 273, 257  
 Partridge R. B., Peebles P. J. E., 1967, *ApJ*, 147, 868  
 Pierce M. J., et al., 1994, *Nat*, 371, 385  
 Pozzetti L., Bruzual A. G., Zamorani G., 1996, *MNRAS*, 281, 953 (PBZ96)  
 Roche N., Shanks T., Metcalfe N., Fong R., 1996, *MNRAS*, 280, 397 (RSMF96)  
 Salpeter E. E., 1955, *ApJ*, 121, 161  
 Saracco P., Chincarini G., Iovino A., 1996, *MNRAS*, 283, 865  
 Scalo J. M., 1986, *Fundam. Cosmic Phys.*, 11, 1  
 Schade D., Barrientos L. F., López-Cruz O., 1997, *ApJ*, 477, L17  
 Schechter P., 1976, *ApJ*, 203, 297  
 Shanks T., 1989, in *The Extra-Galactic Background Light*, eds Bowyer S. C., Leinert C., pub Kluwer Academic Publishers  
 Steidel C. C., Giavalisco M., Pettini M., Dickinson M., Adelberger K. L., 1996, *ApJ*, 462, L17  
 Tinsley B. M., 1972, *ApJ*, 173, L93  
 Tóth G., Ostriker J. P., 1992, *ApJ*, 389, 5  
 Wang B., 1991, *ApJ*, 383, L37

Weinberg S., 1972, in *Gravitation and Cosmology*, Wiley, New York  
 Worthey G., 1994, *ApJS*, 95, 107  
 Yoshii Y., Takahara F., 1988, *ApJ*, 326, 1  
 Zwicky F., 1957, in *Morphological Astronomy*, Springer-verlag

This paper has been produced using the Blackwell Scientific Publications  $\text{\TeX}$  macros.